ELSEVIER

Journal of Alloys and Compounds 434–435 (2007) 119–120

Journal of ALLOYS AND COMPOUNDS

www.elsevier.com/locate/jallcom

Structural study of Zr-based metallic glasses

E. Matsubara [a,*], T. Ichitsubo [a], J. Saida [b], S. Kohara [c], H. Ohsumi [c]

[a] *Department of Materials Science & Engineering, Kyoto University, Kyoto 606-8501, Japan*
[b] *Center of Interdisciplinary Research, Tohoku University, Sendai 980-8578, Japan*
[c] *JASRI, SPring-8, Sayo-gun, Hyogo 679-5198, Japan*

Available online 26 September 2006

Abstract

Structures of $Zr_{70}Ni_{20}Al_{10}$, $Zr_{70}Cu_{20}Al_{10}$, $Zr_{70}Cu_{30}$ and $Zr_{70}Ni_{30}$ amorphous alloys were analyzed by high-energy X-ray diffraction. The relatively stable Zr_2Cu amorphous alloy shows a local atom arrangement different from the Zr_2Cu crystalline phase. By contrast, the less stable $Zr_{70}Ni_{30}$ amorphous alloy has a structure similar to Zr_2Ni. In the $Zr_{70}Cu_{20}Al_{10}$ metallic glass, Zr–Al nearest neighbor pairs are introduced in the amorphous structure. In the $Zr_{70}Ni_{20}Al_{10}$ metallic glass, the strong correlation between Zr–Ni pairs is drastically modified by the formation of Zr–Al pairs. The presence of Zr–Al pairs in the ternary alloys suppresses the crystallization and stabilizes the glassy state.

Keywords: Amorphous materials; X-ray diffraction; Thermal analysis; Synchrotron radiation

Bulk metallic glasses were initially found in noble-metal based alloys, such as, Pd–Ni–P, Pt–Ni–P, etc. [1]. Through 1990s, they have been discovered in other multi-component systems without containing either a noble metal or a metalloid element [2]. Their good GFA and reversible glass–liquid transition have attracted considerable attention. In this paper, we will describe the structural characteristics in relation with the thermal stabilities of the binary $Zr_{70}Cu_{30}$ and $Zr_{70}Ni_{30}$ amorphous alloys. The $Zr_{70}Cu_{30}$ amorphous alloy shows the glass transition before crystallization on heating and the $Zr_{70}Ni_{30}$ amorphous alloy directly crystallizes [3]. Then, the structures of the ternary $Zr_{70}Ni_{20}Al_{10}$ and $Zr_{70}Cu_{20}Al_{10}$ metallic glasses were compared with those of the binary alloys. By partial substitution of Al for Cu or Ni in the binary alloys, the thermal stability in the amorphous state is dramatically improved. We will describe the structural characteristics in the binary and ternary amorphous alloys in order to understand the origin of the thermal stability.

$Zr_{70}Cu_{30}$, $Zr_{70}Ni_{30}$ $Zr_{70}Ni_{20}Al_{10}$ and $Zr_{70}Cu_{20}Al_{10}$ amorphous ribbons about 0.03 mm thick and 2 mm wide were prepared by a single roller melt-spinning technique in argon atmosphere. Densities of the amorphous ribbons measured by Archimedes' method are 7.00 g/cm^3 for $Zr_{70}Cu_{30}$, 7.03 g/cm^3 for $Zr_{70}Ni_{30}$, 6.50 g/cm^3 for $Zr_{70}Ni_{20}Al_{10}$ and 6.50 g/cm^3 for $Zr_{70}Cu_{20}Al_{10}$, respectively. Differential scanning calorimetry (DSC) measurements in the $Zr_{70}Cu_{30}$ and $Zr_{70}Ni_{30}$ amorphous alloys were carried out using a standard commercial instrument (Perkin Elmer Diamond DSC) with about 10 mg samples. Heat flow was measured during heating at a constant heating rate (β) up to 500 °C/min. Glass transition and crystallization temperatures, T_g and T_x, determined by the DSC measurements were divided by the liquidus temperature T_l (1280 °C for $Zr_{70}Cu_{30}$ and 1370 °C for $Zr_{70}Ni_{30}$) to calculate reduced glass transition and crystallization temperatures, T_{rg} and T_{rx}, respectively.

Structures of the amorphous alloys were determined by high-energy X-ray diffraction with 61.74 keV at beam line BL04B2 in SPring-8 synchrotron radiation facility. The advantage in the present high-energy diffraction measurements is a large upper limit of about 270 nm^{-1} for Fourier transformation, which reduces a truncation error in Fourier transformation, so that the spatial resolution of RDF is greatly improved.

Fig. 1 shows T_{rg} and T_{rx} versus $\log\beta$. In the thermally stable $Zr_{70}Cu_{30}$ amorphous alloy, T_g is observed at every β. On the other hand, in the less stable $Zr_{70}Ni_{30}$ amorphous alloy, T_g appears only at a very high β above 200 °C/min [4]. The T_{rg} and T_{rx} values can be fitted with an empirical linear relation, $T_{rx,rg} \equiv T_{x,g}/T_l = a_{x,g} + b_{x,g} \log\beta$. The different slopes for T_{rx} and T_{rg} in Fig. 1 evidently show that the glass transition and crystallization are controlled by different kinetic processes. Since the crystallization is controlled by single atom diffusion, the crystallization is largely retarded by a delay of the diffusion at a fast heating rate. A small positive slope for T_{rg} could be attributed to the structural relaxation of the rapidly quenched amorphous ribbons.

* Corresponding author. Tel.: +81 75 753 3569; fax: +81 75 753 5480.
E-mail address: e.matsubara@materials.mbox.media.kyoto-u.ac.jp (E. Matsubara).

0925-8388/$ – see front matter © 2006 Elsevier B.V. All rights reserved.
doi:10.1016/j.jallcom.2006.08.141

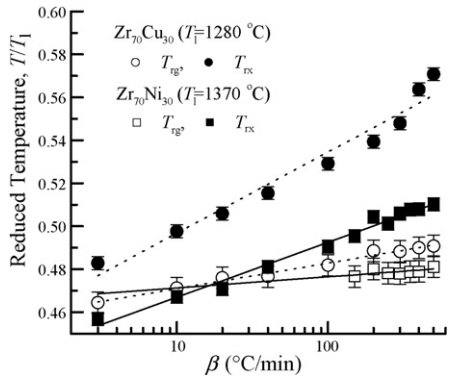

Fig. 1. Reduced glass transition and crystallization temperatures T_{rg} (=T_g/T_l) and T_{rx} (=T_x/T_l) are plotted as a function of log β.

The heating rates β_c and reduced temperature T_{rc} at the intersection of the two T_g and T_x curves are 1.0 °C/min and 0.46 (315 °C) for $Zr_{70}Cu_{30}$ and 17 °C/min and 0.47 (374 °C) for $Zr_{70}Ni_{30}$, respectively [5]. By heating the amorphous alloys at β faster than β_c, we can observe the glass transition. The crystallization takes place prior to the glass transition at β slower than β_c. In $Zr_{70}Cu_{30}$, β_c is less than the commonly used heating rate of about 10 °C/min. On the other hand, in the DSC measurement of $Zr_{70}Ni_{30}$, the amorphous phase is crystallized due to the atom diffusion at β less than β_c, and the diffusion of atoms is suppressed and the glass transition is observed by heating the sample at β more than β_c.

Fig. 2 shows RDFs of the $Zr_{70}Cu_{30}$, $Zr_{70}Cu_{20}Al_{10}$, $Zr_{70}Ni_{30}$ and $Zr_{70}Ni_{20}Al_{10}$ amorphous alloys. Positions of the nearest neighbor pairs are indicated in the figure. The first peak for $Zr_{70}Cu_{30}$ consists of three atom pairs, i.e., Cu–Cu at 0.260 nm, Zr–Cu at 0.284 nm and Zr–Zr at 0.319 nm. These atomic distances are almost equal to those calculated from Goldschmidt radii of Zr (0.160 nm) and Cu (0.128 nm). In contrast, the first peak of the $Zr_{70}Ni_{30}$ amorphous alloy shows a clear split in Fig. 2(b). The peak at 0.32 nm corresponds to Zr–Zr pairs and that at 0.26 nm to Zr–Ni and Ni–Ni pairs. In $Zr_{70}Ni_{30}$, only the atomic distance of Zr–Ni pairs (0.270 nm) is about 5% shorter

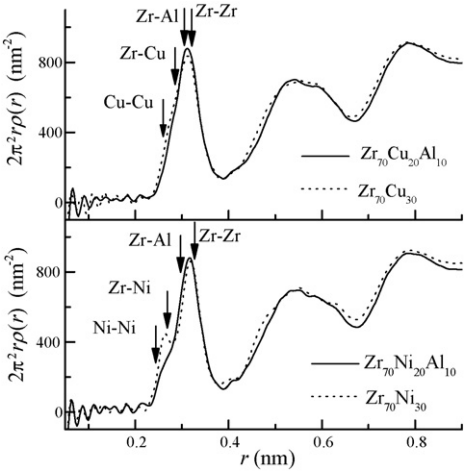

Fig. 2. Radial distribution functions of (a) $Zr_{70}Cu_{20}Al_{10}$ (solid) and $Zr_{70}Cu_{30}$ (dotted), and (b) $Zr_{70}Ni_{20}Al_{10}$ (solid) and $Zr_{70}Ni_{30}$ (doted) amorphous alloys.

than the distance (0.284 nm) calculated from Goldschmidt radii of Zr and Ni (0.124 nm).

On the other hand, the shape of the first peak in $Zr_{70}Cu_{20}Al_{10}$ in Fig. 2(a) resembles that in $Zr_{70}Cu_{30}$, which indicates that the local atom structures or the $Zr_{70}Cu_{20}Al_{10}$ and $Zr_{70}Cu_{30}$ amorphous alloys resemble each other. The peak height for the Zr–Ni pairs at 0.270 nm in Fig. 2(b) is clearly reduced in the $Zr_{70}Ni_{20}Al_{10}$ amorphous alloy by partially substituting Al for Ni.

Crystalline phases produced in $Zr_{70}Cu_{30}$ and $Zr_{70}Ni_{30}$ crystallized in the DSC measurements at every β are tetragonal Zr_2Cu and Zr_2Ni, respectively [5]. In $Zr_{70}Cu_{30}$, the differences of the atomic distances for the Zr–Zr and Zr–Cu pairs between the amorphous and crystalline phases are less than a few %. The difference of Cu–Cu pairs, however, reaches more than 20%. In $Zr_{70}Ni_{30}$, the differences of every pairs are within a few %. Therefore, a much larger change in the Cu–Cu distance is required for the formation of the Zr_2Cu crystalline phase in the $Zr_{70}Cu_{30}$ amorphous alloy. In contrast, the structure of the $Zr_{70}Ni_{30}$ amorphous alloy resembles that of Zr_2Ni. Thus, it is expected that the $Zr_{70}Ni_{30}$ amorphous alloy more easily crystallizes to form the Zr_2Ni phase.

The Zr–Al pairs at the nearest neighbor distance are introduced in $Zr_{70}Cu_{20}Al_{10}$ without large modification of the amorphous structure of $Zr_{70}Cu_{30}$. Thus, the crystallization is suppressed further and the amorphous structure becomes thermally more stable in $Zr_{70}Cu_{20}Al_{10}$. In the $Zr_{70}Ni_{20}Al_{10}$ amorphous alloy, decrease in Zr–Ni pairs leads to a change of its amorphous structure different from Zr_2Ni. Thus, the crystallization in the $Zr_{70}Ni_{20}Al_{10}$ amorphous alloy is suppressed and its thermal stability is improved.

The structures of the $Zr_{70}Ni_{20}Al_{10}$ and $Zr_{70}Cu_{20}Al_{10}$ metallic glasses and the $Zr_{70}Cu_{30}$ and $Zr_{70}Ni_{30}$ amorphous alloys were determined by high-energy X-ray diffraction at SPring-8. Through the measurements of the β-dependence of T_g and T_x in the $Zr_{70}Cu_{30}$ and $Zr_{70}Ni_{30}$ amorphous alloys and their structures in as-quenched and crystallized states, we can conclude that suppression of crystallization is essential in order to prepare a thermally stable amorphous alloy. In the $Zr_{70}Cu_{20}Al_{10}$ and $Zr_{70}Ni_{20}Al_{10}$ metallic glasses, the Zr–Al pairs at the nearest neighbor distance added to the binary systems effectively suppress the crystallization and result in a more thermally stable amorphous structures.

This work was financially supported by Grant-in-Aid for Scientific Research on the Priority Area Investigation of "Materials Science of Bulk Metallic Glasses" from MEXT, Japan. The measurements at SPring-8 were carried out under the approval of the SPring-8 PAC.

References

[1] H.S. Chen, Acta Metall. 22 (1974) 1505–1511.
[2] A. Inoue, Acta Mater. 48 (1) (2000) 279–306.
[3] J. Saida, M. Kasai, E. Matsubara, A. Inoue, Ann. Chimie-Sci. des Materiaux 27 (2002) 77–89.
[4] T. Ichitsubo, E. Matsubara, H. Numakura, K. Tanaka, N. Nishiyama, R. Tarumi, Phys. Rev. B 72 (2005) 052201.
[5] T. Ichitsubo, E. Matsubara, J. Saida, H.S. Chen, Mater. Trans. 46 (10) (2005) 2282–2286.